University of Warsaw
Faculty of Economic Sciences

Working Papers
No. 7/2020 (313)

Price Transmission Across Commodity Markets: Physical to Futures

Gilbert Mbara

Warsaw 2020

UNIVERSITY OF WARSAW
FACULTY OF ECONOMIC SCIENCES
WORKING PAPERS

Price Transmission across Commodity Markets: Physical to Futures

Gilbert Mbara

Faculty of Economic Sciences, University of Warsaw
gmbara@wne.uw.edu.pl

Abstract: Primary commodity prices are generally determined in dual markets: a physical--spot market dominated by supplier--producers and a forward--futures market where consumers, producers and speculators interact. While the futures market operates on an almost continuous basis, the spot market only opens in predetermined short periods of time over which the state of supply and demand is revealed. This poses a challenge for the question of price dynamics: which market leads/follows and where does price discovery occur? We perform an empirical analysis using spot and futures coffee prices and find that most price information originates from the futures markets. Shocks to the spot price are quickly integrated into the market prices, with the effect of the shock quickly dying out or a new equilibrium being attained. A shock to the futures price almost always leads to a permanent change in prices leading to a new equilibrium.

Keywords: Price transmission, futures markets, VECM, Cointegrated VARMA

JEL codes: C5, C51, C58, C32, E32

Acknowledgments: The support of National Science Centre (NSC) grant 2017/27/N/HS4/02037 is gratefully acknowledged. All opinions expressed are those of the authors and have not been endorsed by NSC.

1 Introduction

This study performs an empirical analysis of the transmission of price shocks between physical(spot) and financial(futures) markets using Coffee prices. Our goal is to determine how price transmission occurs between the spot and futures markets in a case where there is a large geographical separation between agents active in the two markets. One such market is that of Green Coffee beans which is produced and sold in several regions of the world away from the financial centers where futures contracts are traded. Unlike commodities produced in advanced countries such as oil, gas, or corn, world coffee production is dominated by producers based in developing countries who have little to no interaction with activities in futures markets where contracts for delivery of their produce is traded. This separation feature of the market provides a unique setting for the evaluation of price discovery and transmission between the physical and financial markets that we examine.

We perform empirical analysis by estimating vector error correction (VECM) and vector autoregressions (VAR) of spot and futures prices for two versions of Coffeer contracts traded in the physical and financial markets: Robusta and Arabica. The Robusta price forward and spot price series form a first difference stationary lag-1 VECM(1) model, with adjustments to price shocks being driven by changes in the futures price equation. Arabica prices are first difference stationary, forming a VAR(2) model but again with price adjustments occurring through the futures price equation. For the VECM(1) Robusta model, shocks to the spot price are quickly integrated to the system and are almost always permanent. Shocks to the futures price have a large impact on prices, leading to a larger price spikes and permanent changes in long-run equilibrium prices. Transmission generally occurs from futures to spot. For the VAR(2) Arabica model, shocks have only temporary effects, dying out within five time periods. The futures price is independent of the spot price with futures price shocks having a larger impact on the futures price itself than on the spot price. The effects of shocks die out within five periods. These results suggest that price discovery occurs in the forward market and information is transmitted from the financial to the physical market.

The remainder of the paper is organized as follows. In the next section, we provide a brief background on the determination of international coffee prices, including the link between spot and futures prices. We also provide a brief literature review on price transmission in dual commodity markets and the econometric/statistical models that have been used in similar studies. Section 3 discusses the VECM($p-1$)/VAR(p) models we use and gives results of unit–root, cointegration and model selection tests we perform. Section 4 concludes.

2 Background

2.1 Determination of International Coffee Prices

Day-to-day physical coffee prices are determined by supply and demand. Price setting criteria are mostly quality (origin), and availability (supply). While each parcel of coffee is unique with regard to its characteristics, flavor and quality; by grouping more or less comparable types of coffee together, average prices can be calculated and traded. Indicator prices, published daily by the International Coffee Organization (ICO) in London, represent and track the four main types of coffee available in the international market: Colombian mild arabicas, Other mild arabicas, Brazilian and other natural arabicas, and Robustas. These indicator prices represent spot or cash prices, quoted in the market for coffee that is more or less immediately available (or within a reasonable time-span). The four categories enable the ICO to calculate market prices for these four broad groups and so monitor price developments for each. In addition, using an agreed formula, the ICO publishes a Daily Composite Indicator Price that combines these four into a single price representing "all coffee". This represents the best indication of a current "international price for coffee".

The Nairobi Coffee Exchange is the physical market of coffees from at least five different African countries. While the output sold at the market is not large compared to producers such as Brazil and Ethiopia, the "Columbian Milds" sold at the auction have a 48–54% weight in the calculation of international coffee prices by the ICO.[1] The NCE coffee also have a price premium of 20 US$ on prices of similar grade coffee traded at the International Coffee Exchange.[2] A causal look at the time series of prices from the NCE and the average prices published by the International Coffee Organization suggests co-movement or integration, with NCE prices showing a constant premium.

Futures prices reflect the estimated future supply and demand for a defined average quality of coffee (e.g. Arabica coffee futures prices in New York, Robusta coffee futures prices in London). In these markets, forward trading is used to offset price risk in the green coffee market where different qualities of coffee are traded. Traders therefore link individual prices with the futures price by establishing a price difference, the differential. The differential takes into account (i) differences between an individual coffee and the standard quality on which the futures market is based, (ii) the supply. For example, by combining the New York or London futures price and the differential, one usually obtains the FOB (free on board) price for a particular type of green coffee. This enables the market to simply quote, for example, "Quality X from Country Y for October shipment at New York December plus 5" (US cts/lb). Traders and importers know the cost of shipping coffee from each origin to Europe, the United States, Japan or wherever, and so can easily transform "plus 5" into a price "landed final destination"(see

[1] See Annex 1 in International Coffee Council (2011)

[2] See e.g. Prices Paid to Growers from the International Coffee Exchange Prices Database http://www.ico.org/coffee_prices.asp

Chapter 8 of the International Trade Centre, 2011, monograph for details).

2.2 Related Literature

The analysis of price transmission from futures to spot markets has a long history. Theoretical contributions relating futures trading to physical/spot market prices include, amongst others Zhou (1998); Goldstein, Li and Yang (2014) and Holmberg and Willems (2015). Recent empirical contributions include for instance the studies by Hache and Lantz (2013) and Juvenal and Petrella (2015). However, all these studies have used futures and spot prices that originate from geographically proximate markets.

There are few if any empirical studies that have tested how futures price changes affect the physical market when there is considerable geographical separation between the spot and forward market. For instance, Chen, Kuo and Chen (2010) analyze the relationship between oil futures and the global spot prices for soybean, corn and wheat and find significant relationships. But they note that these relations can be directly linked to the use of the agricultural commodities in the production of bio-fuels which become competitive with crude oil as the price of the latter increases. Similar findings have been made by Ciaian and Kancs (2011) and Gardebroek and Hernandez (2013) among others. Close geographic proximity and/or non-financial trading relationships (such as substitutability between bio-fuels and many energy products) confound most results in the literature and are therefore not fully informative on the transmission of pure financial trading related shocks to physical prices.

The analysis involves the implementation of vector error correction and vector auto regressions. These methods have been applied for instance by Chen, Turnovsky and Zivot (2014) to link inflation rates with commodity prices, by deB. Harris, McInish and Wood (2002) to study trades that permanently move the market in cross–listed equity shares and Hautsch and Huang (2012) on the long- and short-run effects (impacts) of a market order in a for stocks traded in the Euronext-Amsterdam exchange. The VECM methodology allows for the quantification of the effect of a shock in futures prices on the spot price, together with a measurement of the speed of adjustment after the shock through the co-integrating relationship (see e.g. Baillie, Geoffrey Booth, Tse and Zabotina, 2002).

3 Empirical Analysis

3.1 Data Description

The time series analyzed come from three different databases. Spot prices are from two physical auction markets or “exchanges” in East Africa; the Nairobi Coffee Exchange (NCE) and the Moshi Coffee Exchange (MCE). A detailed description of how these data are generated through the auction mechanism is given in Appendix A. The other spot prices come from the IMF database of primary commodity prices, available at imf.org/[3]. The Arabica spot prices are from the International Coffee Organization (ICO), representing the New York cash price; ex-dock in US cents per pound. The Robusta prices are similarly sourced.

The futures prices are sourced from the CHRIS database hosted at the data provider Quandl[4]. The Robusta Coffee Futures price is a non-adjusted price based on spot-month continuous contract calculations using raw data from London International Financial Futures and Options Exchange (LIFFE, – now part of Intercontinental Exchange (ICE) group). The continuous futures contract chains together a series of individual futures contracts that provide a long-term price history that is suitable for our analysis. The Arabica Futures is similarly computed but has quotations in US dollars. To make the data comparable, we turn the Robusta spot prices to dollars per pound: $S_t = 2204 \times S_t'/100$, where S_t' is the price per pound. Table 1 gives details of the contract specifications. The time series are of monthly frequency from June. 1999 to June 2019. Figures 1a and 1b and 1c shows the time variation of the prices we analyze. The shaded regions are United States NBER recession dates.

Table 1: Futures Contracts Specifications

	Robusta	*Arabica*
Symbol	RC	KC
Contract Size	Ten Tonnes	37,500 pounds
Price Quotation	US $ per metric tonne	US Cents
Min. Price Fluctuation	$1/tonne ($10 per contract)	0.05 cent/lb. ($18.75 per contract)
Settlement	Physical Delivery	Physical Delivery

Figure 1a: log Prices: Arabica

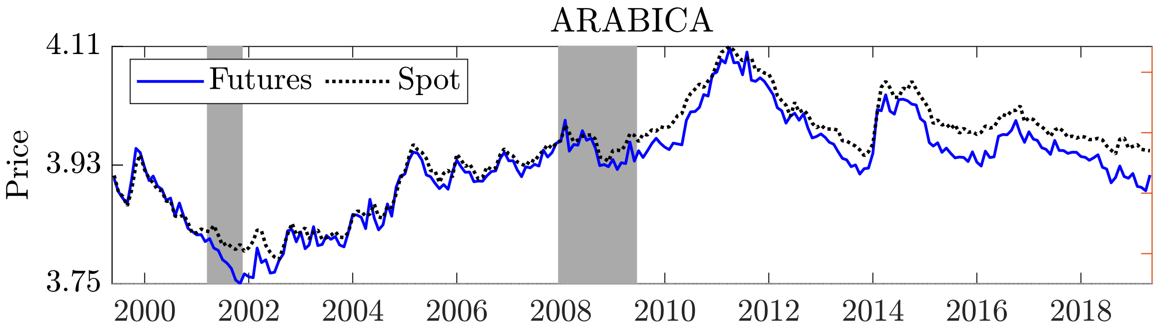

(a) Arabica

The solid(blue) lines represent the nearest maturity futures price, while dotted (black) line represents the spot price. All prices are in logs. The shaded regions are United States NBER recession dates.

[3]https://www.imf.org/en/Research/commodity-prices. The specific data file can be downloaded at the link: https://www.imf.org/ /media/Files/Research/CommodityPrices/Monthly/ExternalData.ashx

[4] https://www.quandl.com/data/CHRIS-Wiki-Continuous-Futures. Quandl Codes: 'CHRIS/LIFFE_RC1' and 'CHRIS/ICE_KC1'

Figure 1b: log Prices: Robusta

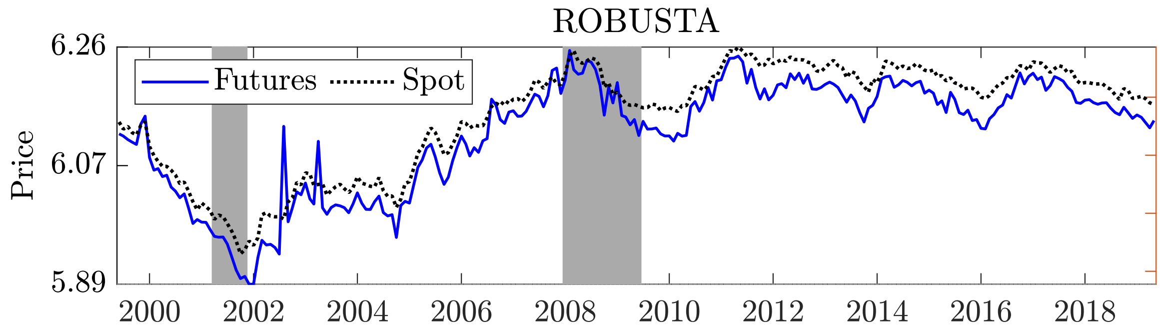

(b) Robusta

The solid(blue) lines represent the nearest maturity futures price, while dotted (black) line represents the spot price. All prices are in logs. The shaded regions are United States NBER recession dates.

Figure 1c: Weekly Prices: Arabica Auction Spot Prices

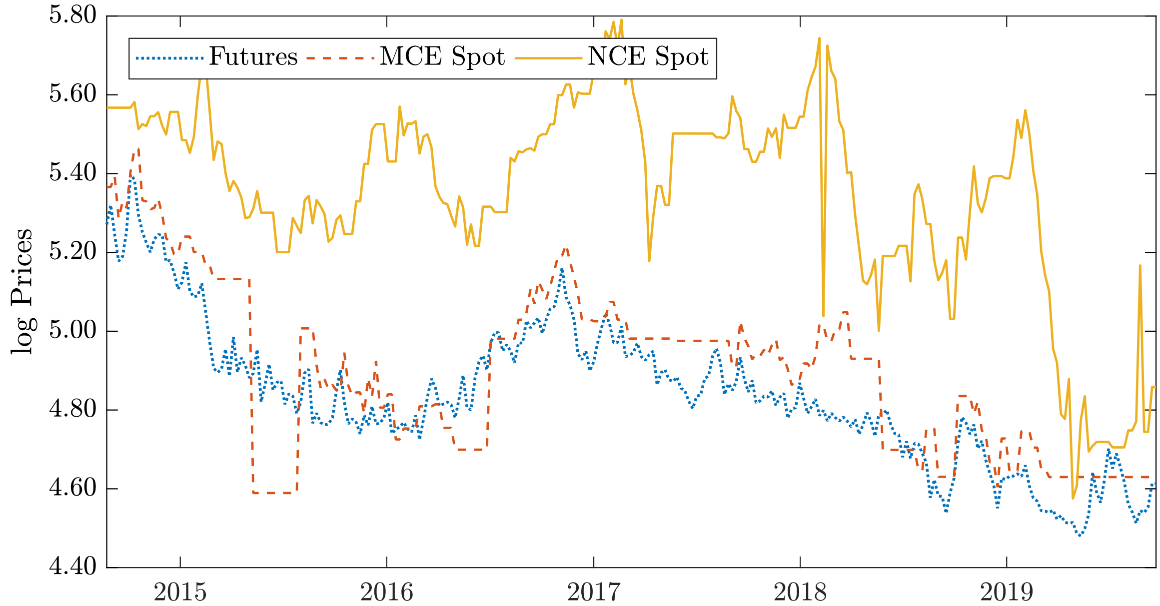

(c) Arabica: NCE and MCE

The solid(gold) line represent NCE spot prices, dotted (blue) line represents the MCE spot price and the dashed (red) line represents the nearest maturity KC futures contract. All prices are in logs. The shaded regions are United States NBER recession dates.

3.2 Cointegration and Error Correction Analysis: Monthly Time Series

Our analysis will therefore involve the following steps:

1. Stationarity / Unit Root Testing

2. Lag - order selection

3. Perform cointegration tests to examine if a cointegration relationship exists.

4. Estimate the VECM with selected lag order.

3.2.1 Unit Root Tests

A univariate time series y_t is said to be integrated if it can be made stationary by differencing. The number of differencing operations required to achieve stationarity defines the order of integration. Most financial/economic time series are integrated of order one. Figures 1a-1b suggest that our prices can be described as a form of random walk or unit root process either with or without a drift. We use the augmented Dickey-Fuller (ADF) tests for each series and summarize the results in Table 2 below. The ADF tests runs a regression of the form:

$$\Delta y_t = \psi y_{t-1} + \sum_{i=1}^{p} \alpha_i \Delta y_{t-i} + u_t, \tag{1}$$

with the null hypothesis $\psi = 0$. Failure to reject the null then leads to the conclusion that the process is integrated of order 1 or $I(1)$. In all cases, we fail to reject the null and conclude that the series are unit root processes. The results shown are for a single lag, but tests using higher order autoregressive terms and alternative specifications including a drift or time trend do not change the conclusions of the tests.

Table 2: ADF Tests

Series	Lags	Test Stat.	Crit. Value	p–value
$f_{t,R}$	0	-0.0956	-1.9421	0.6160
	1	-0.0324	-1.9421	0.6391
$s_{t,R}$	0	0.1119	-1.9421	0.6919
	1	0.1334	-1.9421	0.6998
$f_{t,A}$	0	-0.1235	-1.9421	0.6058
	1	-0.0390	-1.9421	0.6367
$s_{t,A}$	0	0.0992	-1.9421	0.6873
	1	0.1759	-1.9421	0.7154

3.2.2 Cointegration Analysis

When two series are non-stationary and integrated of the same order but with a linear combination that is stationary, then they are cointegrated. We will consider bivariate models containing two $I(1)$ variables f_t and s_t; with the long-run relationship given by:

$$f_t = b_0 + b_1 s_t + u_t, \tag{2}$$

where $b_0 + b_1 s_t$ represents the long-run equilibrium, and u_t represents the short-run deviations from equilibrium, which by assumption is stationary. The long run is represented in Figure 2 by the straight line assuming where $b_1 > 0$. Suppose that the two variables are in equilibrium at point **A**, then from equation 2, the effect of a positive shock in the previous period $(u_{t-1} > 0)$

immediately raises f_t to point **B** while leaving s_t unaffected. For the process to converge back to its long-run equilibrium, there are three possible trajectories.

1. *Adjustments by f_t*: Equilibrium is restored by f_t decreasing toward point **A** while s_t remains unchanged at its initial position. Assuming that the short-run movements in f_t are a linear function of the size of the shock, the adjustment in f_t is given by:

$$f_t - f_{t-1} = a_1 u_{t-1} + v_{1,t} = a_1 (f_{t-1} - b_0 - b_1 s_{t-1}) + v_{1,t} \tag{3}$$

where $a_1 < 0$, is a parameter and $v_{1,t}$ is a disturbance term.

2. *Adjustments by s_t*: Equilibrium is restored by s_t increasing toward point **C** while f_t remains unchanged at its initial position. Assuming that the short-run movements in s_t are a linear function of the size of the shock, the adjustment in s_t is given by:

$$s_t - s_{t-1} = a_2 u_{t-1} + v_{2,t} = a_2 (f_{t-1} - b_0 - b_1 s_{t-1}) + v_{2,t} \tag{4}$$

where $a_2 > 0$, is a parameter and $v_{2,t}$ is a disturbance term.

3. *Adjustments by both f_t and s_t*: Equations (3) and (4) are both in operation and equilibrium is restored towards point **D**. The strengths of the adjustment depend on the size of the coefficients a_1 and a_2.

Equations (3) and (4) represent a VECM where the two variables revert to equilibrium in the next period following a shock. The coefficients a_1 and a_2 are the error correction parameters. The VECM can be rewritten as the VAR subject to cross-equation restrictions since both variables are governed by the same long-run equation. The VAR representation is:

$$\begin{bmatrix} \Delta f_t \\ \Delta s_t \end{bmatrix} = \begin{bmatrix} -a_1 b_0 \\ -a_2 b_0 \end{bmatrix} + \begin{bmatrix} a_1 \\ a_2 \end{bmatrix} \begin{bmatrix} 1 & -b_1 \end{bmatrix} \begin{bmatrix} f_{t-1} \\ s_{t-1} \end{bmatrix} + \begin{bmatrix} v_{1,t} \\ v_{2,t} \end{bmatrix}, \tag{5}$$

which can be expressed as:

$$\begin{bmatrix} f_t \\ s_t \end{bmatrix} = \begin{bmatrix} -a_1 b_0 \\ -a_2 b_0 \end{bmatrix} + \begin{bmatrix} 1+a_1 & -a_1 b_1 \\ a_2 & 1-a_2 b_1 \end{bmatrix} \begin{bmatrix} f_{t-1} \\ s_{t-1} \end{bmatrix} + \begin{bmatrix} v_{1,t} \\ v_{2,t} \end{bmatrix},$$
$$Y_t = \mu + \Phi_1 Y_{t-1} + v_t. \tag{6}$$

This defines VAR(1) with two restrictions on the parameters. In an unconstrained form, the intercepts μ has two parameters while the autocorrelation matrix Φ_1 has four, for a total of six parameters. The model equation (6) consists of just four parameters $\{b_0, b_1, a_1, a_2\}$, so we have 6 - 4 = 2 restrictions.

Accounting for autocorrelation of v_t, the VAR in (6) can be extended to include p lags: $\Phi(L)y_t = \mu + v_t$, where $\Phi(L) = I_N - \Phi_1 L - \cdots - \Phi_p L^p$ is a polynomial in the lag operator L.

Figure 2: Graphical Detection of the Rank

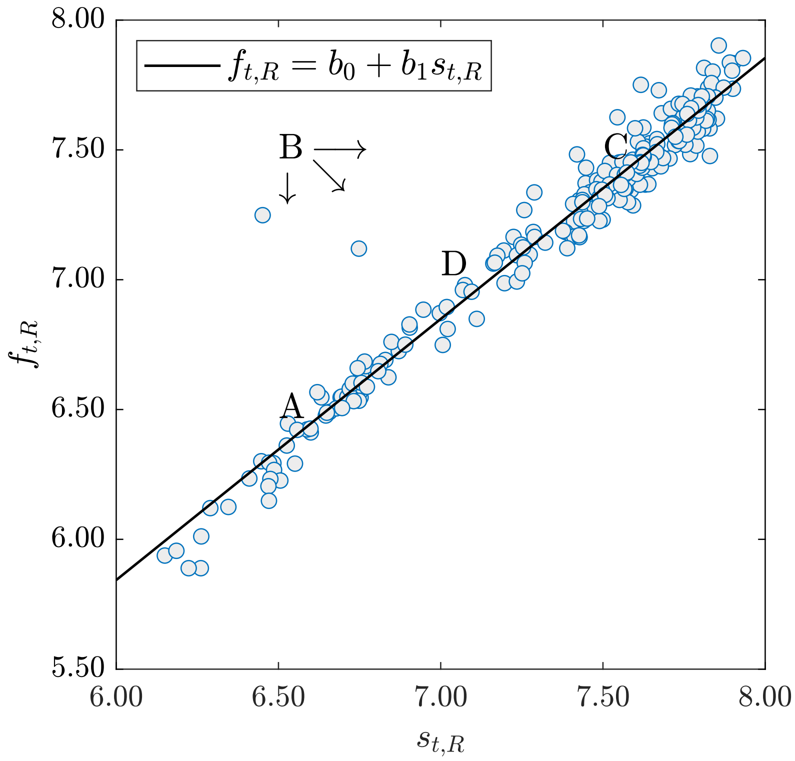

Phase diagram demonstrating a vector error correction model with scatter plot of log futures and log spot price showing potential long–run relationship between the series and their cointegration rank.

The resulting VECM has $p-1$ lags given by:

$$\Delta Y_t = \mu - \Phi(1)Y_{t-1} + \sum_{j=1}^{p-1} \Gamma_j \Delta Y_{t-j} + v_t, \tag{7}$$

where $\Phi(1) = I_N - \Phi_1$ and v_t is $(N \times 1)$. In our case $N = 2$, but in the special case where $N = 1$, then (7) reduces to the Dickey–Fuller regression (1). The operation linking the VAR(p) to the VECM($p-1$) (7) is the Nelson–Beveridge decomposition of the polynomial $\Phi(L)$ as: $\Phi(L) = \Phi(1)L + \Gamma(L)(1-L)$.

Since the vector of prices in Y_t are I(1), then Y_t is cointegrated if there exists a $N \times r$ full column rank matrix B with $1 \leq r < N$, such that the r linear combinations $B'Y_t = u_t$ are I(0). In matrix notation the cointegrating system is given by:

$$\begin{bmatrix} 1 \\ -b_1 \end{bmatrix}' \begin{bmatrix} f_t \\ s_t \end{bmatrix} = \begin{bmatrix} u_t \\ 0 \end{bmatrix} \quad \equiv \quad B'Y_t = u_t \tag{8}$$

where we have assumed that there is one long run equilibrium relationship between f_t and s_t. The dimension r is the cointegrating rank and the column(s) of B the cointegrating vector(s). Figure 2 with the Robusta prices suggests a rank of $r = 1$ with $N - r = 2 - 1 = 1$ common trend.

If Y_t is generated by (7) and if $\Phi(1) = I_2 - \Phi_1$ has reduced rank $r = 1$, with $\Phi(1) = -AB'$

for $1 = r < N = 2$ where A and B are each $(N \times r)$ matrices with full column rank, then by the Granger representation theorem, Y_t is I(1) and $B'Y_t$ is I(0) with cointegrating vector(s) given by the column(s) of B. Otherwise if $\Phi(1)$ has zero rank $r = 0$, then $\Phi(1) = 0$ and Y_t is I(1) and not cointegrated. In our case with $N = 2$, $r = 1$, we have:

$$\Phi(1) = -AB' = -\begin{bmatrix} a_1 \\ a_2 \end{bmatrix} \begin{bmatrix} 1 \\ -b_1 \end{bmatrix}' \tag{9}$$

so that the VECM in equation (7) is subject to the cointegrating restriction (9) is given by:

$$\Delta Y_t = \mu - AB'Y_{t-1} + \sum_{j=1}^{p-1} \Gamma_j \Delta Y_{t-j} + v_t. \tag{10}$$

3.2.3 Lag Order Selection

Performing the cointegration test requires the determination of the lag order p in equation (6) and (7). To obtain the optimal lag, we estimate various versions of (6) and use standard information criteria to select the best model. Since the data shown in Figures 1a and 1b show time trends, we complement (6) with deterministic time trends:

$$Y_t = \mu + \delta t + \Phi_1 Y_{t-1} + v_t, \quad \text{where} \quad \delta = [\delta_1, \delta_2]' \text{ and } t = [1, 2, \ldots, T]'.$$

We present the results of the test in Table 3 below. The AIC and BIC values are for models of lag 1 to 4, with and without intercepts and/or time trends as indicated by the values allocated to μ, δ; 1 for true and 0 for false. The AIC and BIC results agree on a maximum of 2 lags but disagree on the best form of the model in terms of inclusion intercepts and linear time trends. Since the constants μ are all insignificant at 5% level and the time trends are all insignificant, we adopt the model without intercepts and time trends in specifying the VAR(p).

Table 3: VAR Lag–order selection

		Model											
		$\mu = 1, \delta = 1$				$\mu = 0, \delta = 1$				$\mu = 0, \delta = 0$			
	lag$-p$	1	2	3	4	1	2	3	4	1	2	3	4
1	AIC	-1131	-1144	-1133	-1128	-1131	-1144	-1133	-1128	-1117	-1139	-1130	-1128
	BIC	-1103	-1102	-1077	-1058	-1103	-1102	-1077	-1058	-1103	-1112	-1088	-1072
2	AIC	-1291	-1404	-1400	-1390	-1291	-1404	-1400	-1390	-1251	-1397	-1395	-1386
	BIC	-1263	-1362	-1345	-1320	-1263	-1362	-1345	-1320	-1237	-1370	-1354	-1331

3.2.4 Cointegration Tests

We use Johansen tests to assess the null hypothesis $H(r)$ of cointegration rank less than or equal to r among the N time series in $Y = [f_t, s_t]'$ against the alternative $H(r+1)$ (maximum eigenvalue test). The tests also produce maximum likelihood estimates of the parameters in a vector error-correction (VEC) model of the cointegrated series. The test statistics are computed as $-T\log(1-\lambda_{r=1})$ using the effective sample size T and ordered estimates of the eigenvalues of $\Phi(1) = AB', \lambda_1 > \cdots > \lambda_d$, where $d = N$.

Table 4: Cointegration Tests

Robusta					
r	h	Test Stat.	Crit. Value	$p-$value	eig. Val
0	1	58.9109	20.2619	0.0010	0.2148
1	0	1.3482	9.1644	0.8997	0.0056
Arabica					
r	h	Test Stat.	Crit. Value	$p-$value	eig. Val
0	0	12.4745	20.2619	0.4509	0.0409
1	0	2.5469	9.1644	0.7009	0.0106

The results in Table 4 show that the series with Robusta prices are cointegrated with $r = 1$, while the Arabica series are not. The column labeled h shows the cointegrating rank from the test. By the Granger representation theorem, we can conclude that Y_t is $I(1)$ with $\Phi(1) = AB'$ for Robusta prices and that Y_t is $I(1)$ with $\Phi(1) = 0$ for Arabica prices. Using results from the lag-order selection process in Table 3, we convert the VAR(2) model to a VECM(1) for the Robusta prices, but proceed to perform further analysis of Arabica prices using a VAR(p) in first differences.

3.2.5 Impulse Response Functions

Table 5 gives parameter estimates of the VECM(1) model for Robusta prices. In rows labeled AB_{ij} are the coefficients of the impact matrix AB' in equation (7). The adjustment coefficient a_2 is insignificant, which suggests that adjustments to any shocks to equilibrium occur through the futures price. This is further shown in the impulse analysis tracing the effects of shocks to either series on the trajectory of prices. The IRFs in Figure 3 show responses using orthogonalized, one-standard-deviation innovation shocks. For this series, the impact of a shock on prices are almost always permanent. Shocks to s_t are quickly incorporated into a new long-run equilibrium after about 5 months. A shock to the futures price has a larger impact on the spot price, suggesting price discovery occurs in the financial rather than physical market.

In the case of Arabica prices, we obtain a final model with $p = 2$ lags, no intercepts or

Table 5: Parameter Estimates: VECM(1) – Robusta

Parameter	Estimate	S.E.	p–value
μ_1	−0.1123	0.0184	0.0000
μ_2	−0.0020	0.0081	0.8012
a_1	0.0526	0.0078	0.0000
a_2	0.0013	0.0034	0.6985
AB'_{11}	−0.6824	0.1009	0.0000
AB'_{21}	−0.0173	0.0446	0.6985
AB'_{22}	0.6838	0.1012	0.0000
AB'_{21}	0.0173	0.0447	0.6985
$\Gamma_{1,11}$	−0.0253	0.0789	0.7484
$\Gamma_{1,21}$	0.1399	0.0348	0.0001
$\Gamma_{1,12}$	0.1691	0.1484	0.2546
$\Gamma_{2,21}$	0.0780	0.0656	0.2338
log L	578.2356		
T	238		

Figure 3: Impulse Response Functions – Robusta Prices

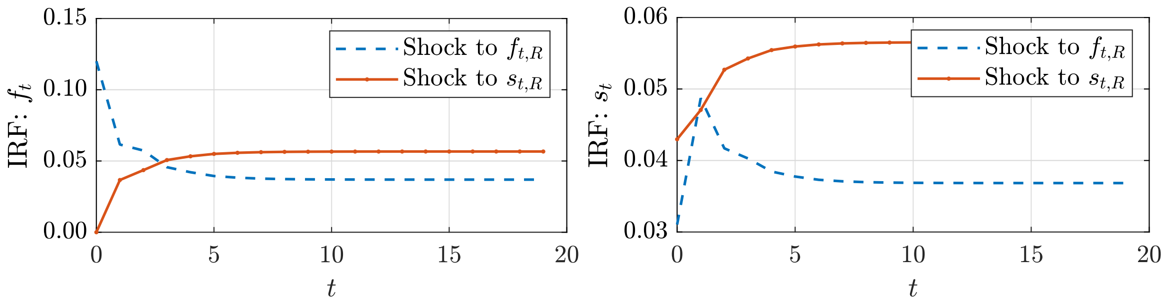

(a) Orthogonalized IRF of f_t (b) Orthogonalized IRF of s_t

time trends but where the lag 2 coefficient matrix has a single estimate $\Gamma_{2,21}$. Table 6 gives the parameter estimates for the VAR(2), after removing the insignificant coefficients and re-estimating the model. These results show that spot prices have no direct impact on futures prices: $\Gamma_{j,12} = 0, \forall j$, but the futures market has impact on the spot market – price discovery therefore takes place in the forward rather than the physical market. Impulse response analysis show the effects of shocks to either series on the trajectory of prices. The IRFs in Figure 4 show responses using orthogonalized, one-standard-deviation innovation shocks. The impact of shocks to s_t on f_t is zero (panel (a), solid line). Shocks to f_t tend to have a larger impact on s_t than its own shocks, again suggesting that price discovery occurs in the futures rather than the spot market.

Table 6: Parameter Estimates: VAR(2) – Arabica

Parameter	Estimate	S.E.	p–value
$\Gamma_{1,11}$	-0.1305	0.0646	0.0435
$\Gamma_{1,21}$	0.5314	0.0480	0.0000
$\Gamma_{1,22}$	-0.3620	0.0605	0.0000
$\Gamma_{2,21}$	0.1211	0.0359	0.0007
log L	702.5842		
T	237		

Figure 4: Impulse Response Functions – Arabica Prices

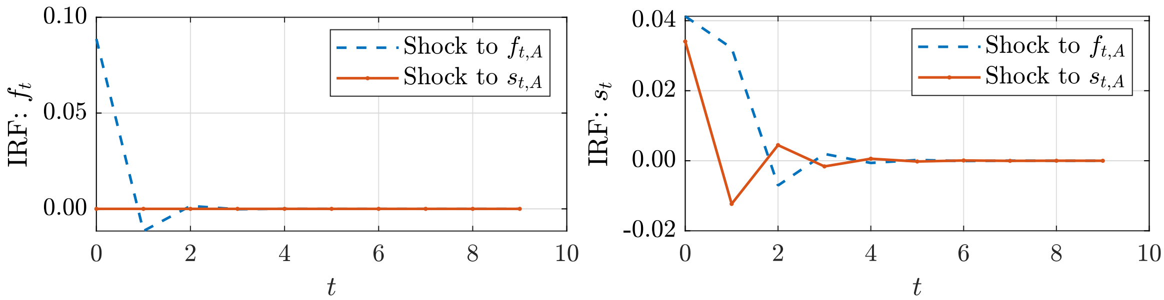

(a) Orthogonalized IRF of f_t (b) Orthogonalized IRF of s_t

3.3 Cointegrated VARMA Analysis: Weekly Time Series

As seen in Figure 1c, the average NCE prices show highly cyclical behavior while the MCE data show more unit root like process variation. This calls for the estimation of a model that can capture these features of the data, for which we use the Cointegrated VARMA.

Following the notation of (6), let the $N-$dimensional process Y_t follow the VARMA(p,q) model:

$$\Phi(L)Y_t = \Theta(L)v_t \tag{11}$$

where $\Phi(L) = \Phi_0 + \Phi_1 L + \Phi_2 L^2 + \cdots + \Phi_p L^p$ and $\Theta(L) = \Theta_0 + \Theta_1 L + \Theta_2 L^2 + \cdots + \Theta_q L^q$ are matrix polynomials, $\Phi_0 = \Theta_0$, Φ_0 is lower triangular with ones in the main diagonal. Following the notation in (7), we assume that the matrix defined by

$$\Pi = -AB' = \Phi(1),$$

has rank r such that $0 < r < N$ and that there are exactly $N - r$ roots in the model equal to one. When the model (11) satisfies these two conditions, it is called a cointegrated VARMA model with cointegration rank equal to r. The error correction form corresponding to the model (11) is:

$$\Gamma(L)\nabla Y_t = \Pi Y_{t-1} + \Theta(L)v_t, \tag{12}$$

where $\nabla = I_N - LI_N$, $\Gamma(L) = \Gamma_0 + \sum_{i=1}^{p-1} \Gamma_i L^i$ and the Γ_i matrices are defined by $\Gamma_0 = \Phi_0$ and

$$\Gamma_i = - \sum_{j=i+1}^{p} \Phi_j, \quad i = 1, \ldots, p-1.$$

It follows from (12) that $B'Y_{t-1}$ is stationary since all the terms in this equation are different from ΠY_{t-1} are stationary. There are therefore r cointegration relations in the model, which are given by $B'Y_{t-1}$.

The model (11) can be written as: $\Phi^*(L)D(L)Y_t = \Theta(L)v_t$, where $D(L) = I_N - U_1 L$ is the *differencing* matrix polynomial, defined using the idempotent symmetric matrix $U_1 = B_\perp \left(B'_\perp B_\perp\right)^{-1} B'_\perp$. $D(L)$ contains all the unit roots in the model and $\Phi^*(L)$ has all roots outside the unit circle, so we obtain the stationary series:

$$D(L)Y_t = [\Phi^*(L)]^{-1} \Theta(L)v_t. \tag{13}$$

We can consequently estimate the VARMA using in differences once we know the polynomial $D(L)$. We proceed by estimating the VARMA in the form (13) first obtaining the matrix B, and the differencing matrix polynomial $D(L)$, then estimate a VARMA for the differenced series $D(L)Y_t$. We implement the model using the SSMATLAB toolbox developed by Victor Gomez Gomez (2019).

3.3.1 Unit Root Tests

We estimate the model (13) for the three time series shown in Figure 1c: $Y_t = [f_t, s_t^{MCE}, s_t^{NCE}]'$; the superscripts denoting the sources of the spot prices. We apply the CRC criterion to the multivariate Y_t series to obtain the number of unit roots. The criterion is a multivariate generalization to the univariate test described in Gómez (2013). Using this criterion, we find two unit roots. We therefore proceed to perform a VAR lag order selection then estimate a cointegrated VARMA(p,q) model with rank imposed (we impose the condition that there is one cointegrating relationship between the three variables in the vector Y_t).

3.3.2 Lag–order & VARMA(p,q) Estimates

We first perform a lag-order identification of the the VAR version of model (11). This involves estimation of a saturated model with many parameters with progressive reduction of lag–order. We obtain log–likelihoods from this process, perform LR tests and select the best model using standard information criteria. The results are displayed in Table 7. Selected orders by AIC, BIC and LR are 2, 1, and 2 respectively. We therefore proceed with a model with $p = 2$. A similar process for the differenced series gives lag order of unity.

We therefore proceed to estimate a model with 2 lags when in the form (11) or 1 lag in the

Table 7: VARMA lag–order selection

Lags	AIC	BIC	LR	$p-$value
0	18.6557	18.6557	0.0000	0.0000
1	13.2459	13.3699	1389.0765	0.0000
2	13.1675	13.4154	37.1274	0.0000
3	13.1799	13.5517	14.2009	0.1154
4	13.2144	13.7102	8.6130	0.4737
5	13.2502	13.8699	8.2088	0.5133
6	13.2663	14.0099	12.8008	0.1718
7	13.2810	14.1486	12.9694	0.1640
8	13.3203	14.3118	7.0787	0.6289

form (13). The estimation results into the following model parameter values:

$$\mu = \begin{bmatrix} 0.3704 \\ -3.5754 \\ -0.4221 \end{bmatrix}, \qquad AB' = \begin{bmatrix} -0.0400 \\ 0.1737 \\ -0.0123 \end{bmatrix} \begin{bmatrix} 1.0000 \\ -0.9856 \\ 0.1147 \end{bmatrix}',$$

and with the AR(1) coefficient matrix:

$$\Gamma_1 = \begin{bmatrix} 0.0229 & 0.0172 & -0.0122 \\ -0.2283 & 0.0123 & -0.0083 \\ -0.2262 & 0.1811 & 0.3644 \end{bmatrix}.$$

4 Conclusion

In this study, we sought to determine how equilibrium prices are determined for a commodity where the physical–spot and financial-futures markets are fully separated. This separation occurs in the market for Coffee because a large share of production occurs in countries with no well developed financial markets. This separation allows for the testing of the location of price discovery and the direction of information transmission across/between the markets. We have found that for Coffee prices, price discovery occurs mostly in the futures markets. One potential explanation for this result is that the futures markets operate continuously, while the spot markets only open at discrete time intervals. It then follows that any shocks to supply and demand are incorporated into the futures price in the intervening periods between spot market events and therefore the futures price always leads the spot price.

References

Baillie, R. T., Geoffrey Booth, G., Tse, Y. and Zabotina, T.: 2002, Price discovery and common factor models, *Journal of Financial Markets* **5**(3), 309–321. doi:10.1016/S1386-4181(02)00027-7. (cited on page 3)

Chen, S.-T., Kuo, H.-I. and Chen, C.-C.: 2010, Modeling the relationship between the oil price and global food prices, *Applied Energy* **87**(8), 2517–2525. doi:10.1016/j.apenergy.2010.02.020. (cited on page 3)

Chen, Y. C., Turnovsky, S. J. and Zivot, E.: 2014, Forecasting inflation using commodity price aggregates, *Journal of Econometrics* **183**(1), 117–134. doi:10.1016/j.jeconom.2014.06.013. (cited on page 3)

Ciaian, P. and Kancs, D.: 2011, Interdependencies in the energy-bioenergy-food price systems: A cointegration analysis, *Resource and Energy Economics* **33**(1), 326–348. doi:10.1016/j.reseneeco.2010.07.004. (cited on page 3)

deB. Harris, F. H., McInish, T. H. and Wood, R. A.: 2002, Security price adjustment across exchanges: an investigation of common factor components for Dow stocks, *Journal of Financial Markets* **5**(3), 277–308. doi:10.1016/S1386-4181(01)00017-9. (cited on page 3)

Gardebroek, C. and Hernandez, M. A.: 2013, Do energy prices stimulate food price volatility? Examining volatility transmission between US oil, ethanol and corn markets, *Energy Economics* **40**, 119–129. doi:10.1016/j.eneco.2013.06.013. (cited on page 3)

Goldstein, I., Li, Y. and Yang, L.: 2014, Speculation and hedging in segmented markets, *Review of Financial Studies* **27**(3), 881–922. doi:10.1093/rfs/hht059. (cited on page 3)

Gómez, V.: 2013, A Strongly Consistent Criterion to Decide Between I(1) and I(0) Processes Based on Different Convergence Rates, *Communications in Statistics - Simulation and Computation* **0918**(1). doi:10.1080/03610918.2012.679760. (cited on page 13)

Gomez, V.: 2019, *Linear Time Series with MATLAB and OCTAVE*, Springer International Publishing. (cited on page 13)

Hache, E. and Lantz, F.: 2013, Speculative trading and oil price dynamic: A study of the WTI market, *Energy Economics* **36**, 334–340. doi:10.1016/j.eneco.2012.09.002. (cited on page 3)

Hautsch, N. and Huang, R.: 2012, The market impact of a limit order, *Journal of Economic Dynamics and Control* **36**(4), 501–522. doi:10.1016/j.jedc.2011.09.012. (cited on page 3)

Holmberg, P. and Willems, B.: 2015, Relaxing competition through speculation: Committing to a negative supply slope, *Journal of Economic Theory* **159**(PA), 236–266. doi:10.1016/j.jet.2015.06.004. (cited on page 3)

International Coffee Council: 2011, Rules on Statisitics Indicator Prices, *Technical report*. (cited on page 2)

International Trade Centre: 2011, *The Coffee Exporter's Guide*, Vol. 1211. (cited on page 3)

Juvenal, L. and Petrella, I.: 2015, Speculation in the Oil Market, *Journal of Applied Econometrics* **30**(4), 621–649. doi:10.1002/jae.2388. (cited on page 3)

Zhou, Z.: 1998, An equilibrium analysis of hedging with liquidity constraints, speculation, and government price subsidy in a commodity market, *Journal of Finance* **53**(5), 1705–1736. doi:10.1111/0022-1082.00069. (cited on page 3)

Appendix

A NCE Auction Data Acquisition and Aggregation

This section gives a description of the data available for analysis from the NCE. It forms part of the paper entitled *Hedging under Price and Demand Risk* funded by the NCN.[5]

A.1 Seller Side Data

Sellers information at the NCE is available through their catalogues. Every week, before the auction, sellers submit a detailed description of the lots of coffee they will have on sale. The catalogues includes standard identifying information such as seller name and date of intended auction/sale. Since the product is sold in lots, with each lot potentially being from a different region, harvest area and/or mill, among other characteristics, the sales are organized per lot, each of which presents product of different quality/grade and quantity. For each lot, a unique ID is issued by the "warehouse-men" and a descriptive "mark" added (and also recorded on 2.5kg the sample bags). Finally grade, quantities on offer and packaging information is included. Table 8 shows a sample catalogue from available to buyers before the auction.

Table 8: Typical Seller Catalogue

SALE No. N.C.E. 1
THE NAIROBI COFFEE EXCHANGE
THROUGH THIKA COFFEE MARKETING LIMITED
WILL OFFER BY AUCTION
1,045 Bags On Tuesday 2nd OCTOBER 2018
at 9.00 a.m.
AT THE EXCHANGE HALL
Wakulima House
NAIROBI
1,045 Bags of Kenya Coffee
Prompt Date 9TH OCTOMBER 2018

LOT	MARK	GRADE	BAGS	PKT	WEIGHT	SALE	SEASON
601	41TK0025/MUKURWE-ESTATE	T	11	8	668	1	2018/19
602	48TK0065/POINT-MZURI	T	16	59	1019	1	2018/19
603	51TK2004/T/BULK	T	15	40	940	1	2018/19
604	51TK2005/T/BULK	T	13	13	793	1	2018/19

[5]The support of National Science Centre grant 2017/27/N/HS4/02037 is gratefully acknowledged. All opinions expressed are those of the author and have not been endorsed by the National Science Centre.

A.2 Buyer Side Data

Buyers have access to the the sellers' catalogues before the auction. Auctions are held every Wednesday, from 9 AM and may last from 6 to 8 hours, depending on the number of lots on offer and how active the bidding is during the sale of each individual bid. There are 80 different "buyer desks" where bids are submitted through a set of buttons available at each desk. The following information is collected at every sale: a transaction number, lot number, season, marks, grade, sale number (of the season), bags and weight bought, buyer code, price, seat number (of buyer in auction hall), agent code (marketing agent or seller identifier) and time. Table 9 shows an extract of the transactions listings file showing information that is relevant to the analysis. Note that the lot numbers, marks ad weight match those of Table 8 as the transactions correspond to the catalogue of the same marketing agent (21/Thika Coffee Mills).

Table 9: Transaction Listing, Sale 1 of 2nd October 2018

TRCN.	LOT	MARKS	WEIGHT	BUYER	PRICE	SEAT	AGENT	TIME
21192	601	41TK0025	668	160	64	40	21	10:42:14
21193	602	48TK0065	1019	160	59	40	21	10:42:44
21194	603	51TK2004	940	74	89	74	21	10:43:21
21195	604	51TK2005	793	74	88	74	21	10:43:43
21196	605	51TK2006	1036	74	97	74	21	10:44:13

A.3 Aggregation

For each Sale (auction day), the price and quantity data are aggregated across each lot sale and grade. For time series analysis, quantities are not used, so the price series are the average(mean) prices over all transactions. For robustness check, I also use time series weighted by the quantities sold in per grade. The aggregation is:

$$p_t = \sum_{i=1}^{n} w_i p_{ti},$$

where $w_i = \frac{q_i}{\sum_{i=1}^{n} q_i}$ is the share of grade i in total volume sold on auction day t and n is the number of grades available on that day. For example, for the sale 1 of Oct. 2, 2018, the available grades are $i = \{$AA,AB, C, HE, MH, ML, PB,T, TT, UG1, UG2, UG3$\}$, which gives the percentage weights: {5.0043 35.8280 38.2781 0.8305 0.7999 1.7275 3.7698 5.4829 2.3710 2.6382 2.9485 0.3213}. An alternative aggregation scheme ignores quantities, computing the weights by grade. Under the grades aggregation scheme, the weights would be {12.0419 28.4468 26.5271 1.9197 1.0471 1.7452 6.9808 8.5515 5.2356 3.8394 3.1414 0.5236}.

University of Warsaw
Faculty of Economic Sciences
44/50 Długa St.
00-241 Warsaw
www.wne.uw.edu.pl